

## A Preliminary Measurement of the $\Xi^0 \rightarrow \Sigma^0 \gamma$ Branching Ratio and Asymmetry Parameter

S. Teige, A. Beretvas,<sup>(a)</sup> A. Caracappa,<sup>(b)</sup> T. Devlin, H. T. Diehl, K. Krueger,<sup>(c)</sup> and G. B. Thomson

*Department of Physics and Astronomy, Rutgers—The State University of New Jersey, Piscataway, New Jersey 08854*

P. Border,<sup>(d)</sup> P. M. Ho, and M. J. Longo

*Department of Physics, University of Michigan, Ann Arbor, Michigan 48109*

and

J. Duryea, N. Grossman, K. Heller, M. Shupe,<sup>(e)</sup> and K. Thorne

*School of Physics and Astronomy, University of Minnesota, Minneapolis, Minnesota 55455*

### ABSTRACT

In an experiment performed at Fermilab, we have observed the weak radiative decay  $\Xi^0 \rightarrow \Sigma^0 \gamma$ . From a sample of  $85 \pm 10$  events we have preliminary measurement of the decay branching ratio  $\Gamma(\Xi^0 \rightarrow \Sigma^0 \gamma) / \Gamma(\Xi^0 \rightarrow \Lambda \pi^0) = (3.56 \pm 0.42) \times 10^{-3}$  and the asymmetry parameter  $\alpha_{\Xi} = 0.20 \pm 0.28$

Several attempts to calculate the rates <sup>1-6</sup> and decay asymmetries <sup>1,3-6</sup> of hyperon radiative decays have been made. Predictions for the branching ratio for  $\Xi^0 \rightarrow \Sigma^0 \gamma$  range over almost two orders of magnitude. Table 1 gives a summary of theoretical predictions. A measurement of the parameters for  $\Xi^0 \rightarrow \Sigma^0 \gamma$  will help to further constrain the theoretical calculations since data on  $\Xi^0 \rightarrow \Sigma^0 \gamma$  are sparse. Only an upper limit of  $7 \times 10^{-2}$ , obtained by Yeh <sup>7</sup> *et al.*, has been published.

TABLE I. A summary of theoretical predictions for  $\Xi^0 \rightarrow \Sigma^0 \gamma$ .

Branching Ratio	Asymmetry	Reference
$10 \times 10^{-3}$	-0.9	1
$9.1 \times 10^{-3}$	—	2
$7.2 \times 10^{-3}$	-0.96	4
$5.87 \times 10^{-3}$	-0.58	3
$(2.62-4.58) \times 10^{-3}$	0.81-0.97	6
$1.48 \times 10^{-3}$	-0.30	5
$0.23 \times 10^{-3}$	-0.99	5

The decay  $\Xi^0 \rightarrow \Lambda \pi^0$ ;  $\pi^0 \rightarrow \gamma \gamma$  has a topology identical to  $\Xi^0 \rightarrow \Sigma^0 \gamma$ ;  $\Sigma^0 \rightarrow \Lambda \gamma$  and our trigger was equally sensitive to both so our  $\Xi^0$  sample contained events from both decay chains. The decay chains are kinematically ambiguous over a substantial region of the available phase space due to the finite resolution of our apparatus.

The detector <sup>8</sup> (See Figure 1.) consisted of 3 multiwire proportional chambers (MWPC) followed by an analysis magnet with a 1.6 GeV/c transverse momentum bend followed by three more MWPC's. These chambers were used to reconstruct the vector momenta of charged tracks. The trigger required the coincidence  $\bar{V}1 \cdot S1$  which indicated a neutral particle decay. In addition two scintillator hodoscopes, A and B, were used to select events with a pair of tracks. Two additional scintillation counters, P1 and P2, extended the coverage of the trigger to the most central region of the detector where the protons from  $\Lambda \rightarrow p \pi^-$  were most likely to be found. This requirement served to select events with a visible  $\Lambda \rightarrow p \pi^-$  decay. Following the last MWPC was an array of lead glass blocks. The center block of the array was missing to allow the neutral beam to pass through without initiating showers. The trigger required two separated clusters of blocks, not associated with charged tracks, to have a signal above threshold. This requirement selected events with more than one photon.

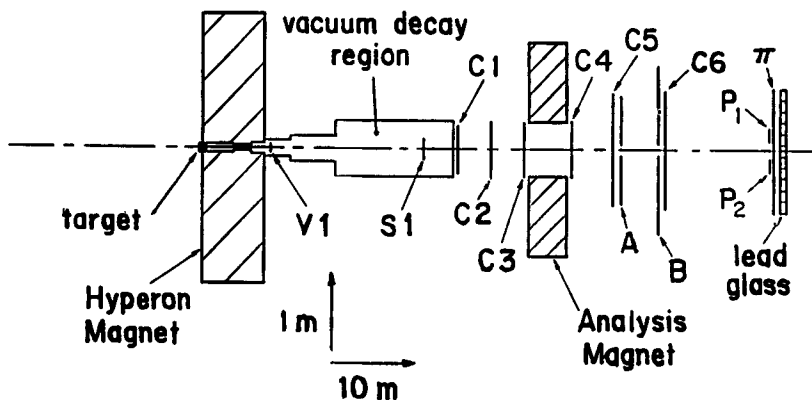


FIG. 1. Plan view of the apparatus showing the 800 GeV/c proton beam, the  $\Xi^0$  production target, Hyperon magnet, scintillation counters S1 and V1, multiwire proportional chambers C1-C6, the A and B scintillator hodoscopes, and the lead glass array .

A total of  $8 \times 10^6$  triggers were recorded. The analysis program read the raw data tapes and reconstructed the charged tracks. Preliminary cuts to select events with a  $\Lambda$  were made as follows: (1) There were exactly two charged tracks of opposite sign reconstructed, (2) the effective mass of the track pair, under the hypothesis  $p^+ \pi^-$ , was within  $10 \text{ MeV}/c^2$  of the  $\Lambda$  mass. Further preliminary cuts to select  $\Xi^0$  candidates were: (1) There were exactly two clusters of hits in lead glass array not associated with charged hits, (2) both clusters had energy larger than 5.6 GeV. A fit was performed to find the  $\Xi^0$  vertex. It was required that a vertex could be chosen along the path of the  $\Lambda$  such that the  $\Lambda \gamma \gamma$  effective mass was equal to the  $\Xi^0$  mass and that this vertex was, within resolution, upstream of the  $\Lambda$  vertex. It was required that the angle  $|\delta|$  between the vector from the target to the decay vertex and the vector along the momentum, be less than 1 mr. The  $\Lambda$  was projected back to the target and the distance squared from the center of the target was required to be larger than  $0.15 \text{ cm}^2$ . This rejected  $\Lambda$ 's not associated with a  $\Xi^0$  decay. The  $\Xi^0$  was projected to the target plane and required to be within 0.6 cm of the target center. It was further required that the direction of the  $\Xi^0$  momentum be within  $1.5 \sigma$  of the average beam direction. To eliminate events with

photons that lost a substantial fraction of their shower energy down the uninstrumented beam hole it was required that the block in each photon cluster with the most energy not be adjacent to the beam hole. These cuts rejected badly reconstructed  $\Xi^0 \rightarrow \Lambda\pi^0$  or those not coming from the target and produced a data sample of 71832  $\Xi^0$  decays. Table 2 summarizes the effects of the cuts on the data sample.

To select  $\Xi^0 \rightarrow \Sigma^0\gamma$  events the requirement  $|m_{\gamma\gamma} - m_{\pi^0}| > 40 \text{ MeV}/c^2$  was imposed. This cut rejected more than 99 % of the  $\Xi^0 \rightarrow \Lambda\pi^0$  events while passing 33 % of the  $\Xi^0 \rightarrow \Sigma^0\gamma$  events. The peak due to the  $\Sigma^0$  was visible in the distribution of  $\Lambda\gamma$  effective masses after this cut was imposed (see Figure 2). The smooth curve in figure 2 is the  $\Lambda\gamma$  effective mass distribution for  $\Xi^0 \rightarrow \Sigma^0\gamma$  events as calculated by our Monte Carlo simulation plus a constant background.

TABLE II. Event selection.

Cut	Events
Trigger	$8 \times 10^6$
Initial Reconstruction	330427
$ \delta $ cut	272347
Cluster timing cut	232236
Reconstructed $\Xi$ points to target	205490
$r^2$ of $\Lambda$	161887
Beam cone cut	113009
No hole clusters	71832
$ m_{\gamma\gamma} - m_{\pi^0} $	240

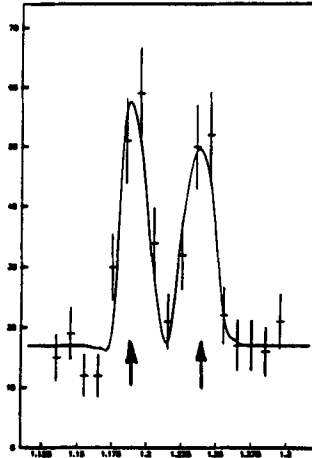


FIG. 2. The  $\Lambda\gamma$  effective distribution. Both combinations of  $\Lambda\gamma$  effective mass are plotted. The arrows show the location of the  $\Sigma^0$  mass and its reflection.

To extract the branching ratio the  $\Lambda\gamma$  effective mass distribution was fitted to a sum

of the  $\Lambda\gamma$  effective mass distribution for  $\Xi^0 \rightarrow \Sigma^0\gamma$  events determined by Monte Carlo calculation and a constant background. Both  $\Lambda\gamma$  combinations were used to fill the distributions since both had narrow distributions for events due to  $\Xi^0 \rightarrow \Sigma^0\gamma$ . The fit yielded  $85 \pm 10$   $\Xi^0 \rightarrow \Sigma^0\gamma$  events over a background of 70 events within  $15 \text{ MeV}/c^2$  of the  $\Sigma^0$  mass with a  $\chi^2/\text{D.F.}$  of 0.9.

The branching ratio could be calculated once the relative acceptance for the two decay modes was known. The acceptance ratio was calculated by subjecting the Monte Carlo samples to the same analysis programs that extracted the data distributions. The overall acceptance for the  $\Xi^0 \rightarrow \Lambda\pi^0$  mode was 3.00 times the acceptance for the  $\Xi^0 \rightarrow \Sigma^0\gamma$  mode. The result was

$$\frac{\Gamma(\Xi^0 \rightarrow \Sigma\gamma)}{\Gamma(\Xi^0 \rightarrow \Lambda\pi)} = \frac{(85 \pm 10) \times 3.00}{71592} = (3.56 \pm 0.42) \times 10^{-3}. \quad (1)$$

The denominator is the number of events passing all cuts but the  $40 \text{ MeV}/c^2$   $\gamma\gamma$  effective mass cut.

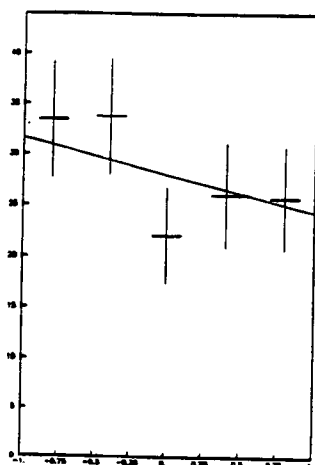


FIG. 3. The distribution of  $\cos \theta$  used to extract the asymmetry parameter. The straight line is the result of the fit.

To calculate the asymmetry, events were selected such that the smallest  $\Lambda\gamma$  effective mass was within  $15 \text{ MeV}/c^2$  of the  $\Sigma^0$  mass. The background subtracted distribution of  $\cos \theta$  was corrected for acceptance by Monte Carlo calculation and fitted to a functional form

$$\frac{dN}{d(\cos \theta)} = N_0(1 - \alpha_\Lambda \alpha_\Xi \cos \theta) \quad (2)$$

where  $\alpha_\Lambda$  was taken to be  $0.642 \pm 0.013$  <sup>9</sup> and  $\theta$  was the angle between the proton and the boost axis of the  $\Sigma^0$  in the rest frame of the  $\Lambda$ . The background was parameterized as

$$\frac{dN}{d(\cos \theta)} = B(1 + \alpha_B \cos \theta) \quad (3)$$

where  $B$  was the number of background events and  $\alpha_B$  was determined by fitting equation 3 to a distribution obtained from events failing the requirement that the  $\Lambda\gamma$  mass be within  $15 \text{ MeV}/c^2$  of the  $\Sigma^0$  mass but passing all other cuts. The asymmetry parameter  $\alpha_{\Xi}$  was found to be  $0.20 \pm 0.28$ . Figure 3 shows the distribution and the result of the fit. Systematic errors were investigated allowing  $\alpha_B$  to vary within the errors of its measurement. The effect of the acceptance correction was investigated by removing the correction from the calculation. Both effects were found to be small compared to the statistical error.

In conclusion, we have observed  $85 \pm 10 \Xi^0 \rightarrow \Sigma^0 \gamma$  events in a sample of 71832  $\Xi^0$  decays. When corrected for acceptance this yields a branching ratio  $\Gamma(\Xi^0 \rightarrow \Sigma^0 \gamma) / \Gamma(\Xi^0 \rightarrow \Lambda \pi^0) = (3.56 \pm 0.42) \times 10^{-3}$ . The asymmetry parameter was measured to be  $\alpha_{\Xi} = 0.20 \pm 0.28$ .

<sup>(a)</sup>Present address: Fermi National Accelerator Laboratory, P.O. Box 500, Batavia, IL 60510

<sup>(b)</sup>Present address: Brookhaven National Laboratory, National Synchrotron Light Source, Upton, NY 11973

<sup>(c)</sup>Present address: Northeastern State University, Division of Natural Sciences and Mathematics, Tahlequah, OK 74464

<sup>(d)</sup>Present address: School of Physics and Astronomy, University of Minnesota, Minneapolis, MN 55455

<sup>(e)</sup>Present address: Department of Physics, University of Arizona, Tucson, AZ 85721

<sup>1</sup> M. Scadron and L. Thebaud, Phys. Rev. **D8**, 2190 (1973).

<sup>2</sup> F. J. Gilman and A. B. Wise, Phys. Rev. **D19**, 976 (1979).

<sup>3</sup> K. G. Rauh, Z. Phys. **C10**, 81 (1981).

<sup>4</sup> M. B. Gavela *et al.*, Phys. Lett. **101B**, 417 (1981).

<sup>5</sup> A. N. Kamal and R. C. Verma, Phys. Rev. **D26**, 190 (1982).

<sup>6</sup> R. C. Verma and Avinash Sharma, Phys. Rev. **D38**, 1443 (1988).

<sup>7</sup> N. Yeh *et al.*, Phys. Rev. **D10**, 3545 (1974).

<sup>8</sup> N. Grossman *et al.*, Phys. Rev. Lett. **59**, 18 (1987),

P. Border, Ph.D. Thesis, University of Michigan, (1988) (Unpublished).

<sup>9</sup> O. E. Overseth and R. F. Roth Phys. Rev. Lett. **19**, 391 (1967),

W. E. Cleland *et al.* Nuc. Phys. **B40**, 221 (1972)